Dalton Transactions

Accepted Manuscript

This is an *Accepted Manuscript*, which has been through the Royal Society of Chemistry peer review process and has been accepted for publication.

Accepted Manuscripts are published online shortly after acceptance, before technical editing, formatting and proof reading. Using this free service, authors can make their results available to the community, in citable form, before we publish the edited article. We will replace this *Accepted Manuscript* with the edited and formatted *Advance Article* as soon as it is available.

You can find more information about *Accepted Manuscripts* in the Information for Authors.

Please note that technical editing may introduce minor changes to the text and/or graphics, which may alter content. The journal's standard Terms & Conditions and the Ethical guidelines still apply. In no event shall the Royal Society of Chemistry be held responsible for any errors or omissions in this *Accepted Manuscript* or any consequences arising from the use of any information it contains.

ROYAL SOCIETY OF CHEMISTRY

www.rsc.org/dalton

Please do not adjust margins

Journal Name

ARTICLE

Ring-tension Adjusted Ethylene Polymerization by Aryliminocycloheptapyridylnickel Complexes

Received 00th January 20xx,
Accepted 00th January 20xx

DOI: 10.1039/x0xx00000x

www.rsc.org/

Fang Huang,[a,b] Zelin Sun,[b] Shizhen Du,[b] Erlin Yue,[b] Junjun Ba,[a,b] Xinquan Hu,*[,a] Tongling Liang,[b] Griselda B. Galland,[c] and Wen-Hua Sun*[,b,d]

The stoichiometric reactions of 5,6,7,8-tetrahydrocycloheptapyridin-9-one (cycloheptapyridin-9-one) with various anilines lead to the corresponding mixtures of 9-aryl-iminocycloheptapyridine and the isomeric 9-arylamino-5,6,7-trihydrocycloheptapyridine derivatives; these compounds further reacted with nickel dichloride to form 9-aryliminocyclo-heptapyridylnickel chlorides, respectively. The new organic compounds were analyzed by the NMR measurements, and all the organic and complex compounds were characterized by the FT-IR spectroscopy and elemental analysis. In addition, the molecular structures of representative nickel complexes **Ni1** and **Ni3**, determined by means of single crystal X-ray diffraction, were found to be the binuclear dimers with the distorted square-pyramidal geometry around the nickel center. On activation with either ethylaluminium sesquichloride ($Et_3Al_2Cl_3$) or methylaluminoxane (MAO), all nickel complex pre-catalysts exhibited high activities of up to 7.80×10^6 gPE·mol^{-1}·(Ni)·h^{-1} toward ethylene polymerization and produced highly branched polyethylenes in narrow polydispersity. The title nickel complexes showed comparable activities with 8-arylimino-5,6,7-trihydroquinolylnickel analogues; whilst both exhibited higher activities than did the 2-iminopyridylnickel analogues due to the enhancement of the ring-tension of cyclic-fused pyridine derivatives.

Introduction

Following the pioneer works of the α-diiminometal (Ni^{2+} or Pd^{2+}) complexes[1] and bis(imino)pyridylmetal (Fe^{2+} or Co^{2+}) complexes,[2] the late-transition metal complex pre-catalysts for ethylene polymerization have been extensively investigated in the past two decades.[3,4] The characteristic features of the resulting polyethylenes are the linearity for both iron and cobalt pre-catalysts[4] and the high level of branches for nickel pre-catalysts.[3] Within the late-transition metal pre-catalysts, there are more reports on nickel complex pre-catalysts[3] comparing with both iron and cobalt complexes.[4] In order to maintain the academic interest and attract research funds from industry, the catalytic systems with potential applications are in high demand for the pilot or industrial processes. Currently, the iron complex pre-catalyst in ethylene oligomerization has successfully scaled up in 500 tons pilot process,[5] moreover, other pilot processes employing iron complex pre-catalysts for polyethylene waxes are being evaluated for the suitability to the pilot process.[6] Regarding the ethylene polymerization by nickel complex pre-catalysts,[3] the resultant polyethylenes commonly show high content of branches, which indicates the unique structural feature similar to polyolefin elastomer (POE) produced by half-metallocene CGC pre-catalysts.[7] The POE materials are widely used in thermal packaging, and applied as shape memory materials, anti-freezing agents, compatilizers as well as the additives for enhancing greasiness or wear resistance. To meet the practical demands set for the catalytic systems, the nickel complex pre-catalysts are adapted through the fine modification of the ligand compounds. Inspired by the nickel-based industrious SHOP process for ethylene oligomerization,[8] various ligands of imino and other heteroatoms such as phosphine,[9] oxygen[10] and nitrogen of imidazole[11] were explored for their nickel complexes, however, these nickel pre-catalysts did not provided catalytic performances as good as α-diiminonickel halides (**A**, Scheme 1).[12] In addition to typical α-diiminonickel halide pre-catalysts,[12] the 2-iminopyridylnickel complex pre-catalysts (**B**, Scheme 1) were also extensively investigated and exhibited high catalytic activities.[13] Furthermore, considering the ring-tension of fused-cyclic frameworks acting as ligands, 8-arylimino-5,6,7-trihydroquinoline derivatives were purposefully designed; and the corresponding nickel complexes (**C**, Scheme 1) acted as the single-site active species with higher activities than the 2-iminopyridylnickel analogues,[13] performing ethylene either oligomerization[14] or

[a] College of Chemical Engineering, Zhejiang University of Technology, Hangzhou 310014, China.
[b] Key laboratory of Engineering Plastics and Beijing National Laboratory for Molecular Science, Institute of Chemistry, Chinese Academy of Sciences, Beijing 100190, China.
[c] Instituto de Química, Universidade Federal do Rio Grande do Sul, Av. Bento Gonçalves 9500, 91501-970 Porto Alegre, Brasil.
[d] State Key Laboratory for Oxo Synthesis and Selective Oxidation, Lanzhou Institute of Chemical Physics, Chinese Academy of Sciences, Lanzhou 730000, China.

† Appendix A. Supplementary material: CCDC 1062047 and 1062048 contain the supplementary crystallographic data for Ni1 and Ni3. These data can be obtained free of charge from The Cambridge Crystallographic Data Centre via www.ccdc.cam.ac.uk/data_request/cif

Dalton Transactions Accepted Manuscript

polymerization[15] on the basis of ligands of 5,6,7-trihydroquinoline derivatives having 2-substitutents or not.

The role of ring strain within ligand framework affects the catalytic performance of the corresponding metal complexes. For example, ethylene polymerization catalyzed by 8-arylimino-5,6,7-trihydroquinolylnickel pre-catalysts[15] was enhanced comparing with the analogues 2-iminopyridylnickel complexes;[13] moreover, the 2,9-diimino-5,6,7,8-tetrahydrocycloheptapyridyl iron complex pre-catalysts[16] showed higher activities than did the 2,6-diiminopyridyliron pre-catalysts[2] and arylimino-5,6,7-trihydroquinolylnickel pre-catalysts,[15] in which the positive results were ascribed to the cause of ring tensions of the fused cycloheptane and cyclohexane. Within this work, the series of 9-arylimino-5,6,7,8-tetrahydrocycloheptapyridine (9-aryl-iminocyclo-heptapyridine) and the isomeric 9-(arylamino)-5,6,7-trihydrocycloheptapyridine derivatives were synthesized and used to form the corresponding 9-arylimino-5,6,7,8-tetrahydrocycloheptapyridylnickel complexes (**D**, Scheme 1). In addition to the characterizations of all the organic compounds and nickel complexes, the molecular structures of the representative nickel complexes **Ni1** and **Ni3** were determined by single crystal X-ray diffraction. Moreover, all the nickel complexes showed high activities towards ethylene polymerization with producing polyethylenes with high branches and narrow polydispersity. Herein we report the syntheses and characterizations of organic compounds and the corresponding nickel complexes; the ethylene polymerization catalyzed by nickel complexes as well as the measurements of the resultant polyethylenes were also conducted.

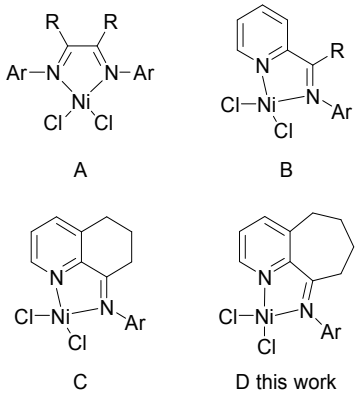

Scheme 1. Representative models of *N*,*N*-bidentate nickel pre-catalysts

Results and Discussion

Synthesis and Characterizations. The condensation reactions of 5,6,7,8-tetrahydrocycloheptapyridin-9-one (cyclohepta-pyridin-9-one) with various anilines were individually conducted to target for 9-aryliminocycloheptapyridine derivatives. In order to achieve the reasonable isolated yields (74 – 83 %, Scheme 2), it was necessary to carry out the reaction in the refluxing chlorobenzene according to the literature procedure.[15a,17] The analyses of these resulting compounds by $^{1}H/^{13}C$ NMR, FT-IR spectroscopy and elemental analysis confirmed the presence of two isomers, 9-aryliminocycloheptapyridine (**L**) and 9-arylamino-5,6,7-trihydrocycloheptapyridine (**L'**), due to the double-bond migration between the cycloheptenamine and iminocyclo-heptance. The NMR results showed the iminocycloheptance (**L**) as the dominant form of lower energy, which is consistent with the literature observations.[15a,16]

The mixture of two organic isomers reacted straightforward with the stoichiometric amount of $NiCl_2$ in the solvent mixture of ethanol and dichloromethane; the corresponding 9-aryliminocycloheptapyridylnickel chloride complexes (**Ni1** – **Ni5**, Scheme 2) were isolated in good to high yields (78 – 93 %), respectively. Their FT-IR spectra illustrated the adsorption of $\nu_{C=N}$ in the region 1607-1613 cm^{-1}, indicating the effective coordination of N_{sp2} atoms with the nickel cation. Unlike to the organic isomers (**L** and **L'**) containing the ν_{N-H} stretching vibrations around 3360 cm^{-1}, the nickel complexes had no signals related to the N-H groups, confirming that the transformation of isomeric enamines **L1'** – **L5'** into the imine analogues **L1** – **L5** occurred during the coordination with the nickel cation. In addition, the single crystals of complexes **Ni1** and **Ni3** were obtained and measured by single crystal X-ray diffraction.

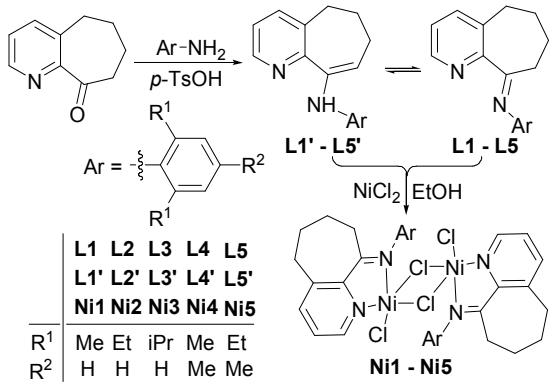

Scheme 2. Synthetic procedures for the organic compounds **L1-L5** and the nickel complexes **Ni1-Ni5**

X-ray Crystallographic Studies. Single crystals of the complexes **Ni1** and **Ni3** suitable for the X-ray diffraction were individually grown by layering diethyl ether on respective solutions in dichloromethane/methanol (v/v=5:1) at room temperature, respectively. Both complexes **Ni1** and **Ni3** turned out to be the chloro-bridged dimer with the distorted square-pyramidal geometry around the nickel cation; such binuclear nickel model was often reported in the bidentate nickel halide complexes.[13,14b,15c] The molecular structures of both **Ni1** and **Ni3** are shown in Figures 1 and 2, respectively, and their selected bond lengths and angles are listed in Table 1.

The distorted square-pyramidal geometry, shown in Figure 1, contains chloride atom (Cl2) at the apex, and the basal plane having elements of two nitrogens (N1 and N2) and two chlorides (Cl1 and Cl3); the nickel (Ni1) is located inside the pyramidal. The Ni-$N_{pyridyl}$ bond (2.044(2) Å) is relatively shorter than the Ni-N_{imino} (2.068(2) Å), which is consistent to the

Dalton Transactions Accepted Manuscript

This journal is © The Royal Society of Chemistry 20xx

observation for the analogue 8-arylimino-5,6,7-trihydroquinolinyl nickel complexes.[15] In addition, the phenyl plane linked to the N_{imino} is almost perpendicular (with the dihedral angle of 88.83°) to the coordinating plane of N1, N2 and Ni atoms. Within the fused cycloheptance, there is a large deviation of the carbon (C9) from the plane of pyridine due to the structural flexibility.[16]

Table 1. Selected Bond Lengths (Å) and Angles (°) for **Ni1** and **Ni3**.

	Ni1	Ni3
Bond lengths (Å)		
Ni(1)-N(1)	2.044(2)	2.038(2)
Ni(1)-N(2)	2.068(2)	2.077 (18)
Ni(1)-Cl(1)	2.381(9)	2.322(8)
Ni(1)-Cl(2)	2.2713(11)	2.278(8)
N(2)-C(11)	1.435(3)	1.451(3)
Ni…Ni	3.453	3.441
Bond angles (°)		
N(1)-Ni(1)-N(2)	78.96(8)	77.99(8)
N(1)-Ni(1)-Cl(1)	167.71(6)	156.13(6)
N(1)-Ni(1)-Cl(2)	91.30(6)	98.92(6)
N(2)-Ni(1)-Cl(1)	94.71(6)	96.99(6)
N(2)-Ni(1)-Cl(2)	100.71(6)	93.89(6)
Cl(1)-Ni(1)-Cl(2)	100.28(3)	104.73(4)
C(1)-N(1)-Ni(1)	125.11(17)	126.53(16)
C(5)-N(1)-Ni(1)	113.07(16)	113.15(16)
C(6)-N(2)-Ni(1)	115.69(16)	113.67(16)
C(11)-N(2)-Ni(1)	125.02(15)	124.04(14)

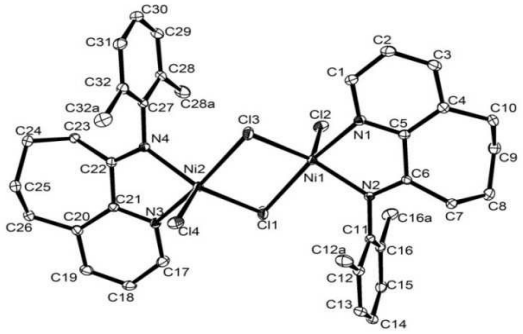

Figure 1. Molecular structure of complex **Ni1** with thermal ellipsoids at 30% probability. Hydrogen atoms were omitted for clarity.

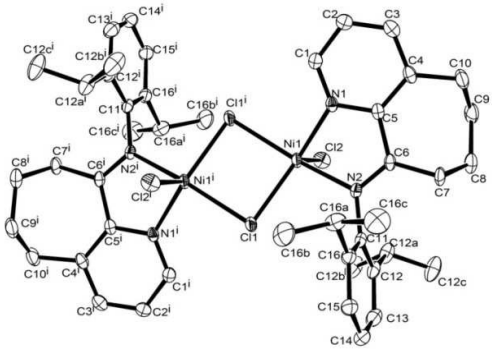

Figure 2. Molecular structure of complex **Ni3** with thermal ellipsoids at 30% probability. Hydrogen atoms were omitted for clarity.

Unlike the complex **Ni1**, complex **Ni3** is a centrosymmetric dimer (Figure 2), but shows the similar coordination feature around nickel atom as in **Ni1**. The Ni-$N_{pyridyl}$ bond (Ni1-N1, 2.038(2)) is slightly shorter than Ni-N_{imino} (Ni1-N2, 2.077(18) Å); and the phenyl plane attached to the N_{imino} atom is near perpendicular to the coordinating plane of N1, N2 and Ni atoms, with a dihedral angle of 81.65°.

Ethylene Polymerization

The catalytic behavior toward ethylene polymerization of the nickel complexes was carefully investigated, including the selection of suitable co-catalysts, the optimum parameters and the measurements regarding resulting polyethylenes.

The selection of the suitable co-catalysts. Complex **Ni3** was used to optimize the polymerization parameters according to the procedure reported.[15] The various alkylaluminum reagents, such as diethylaluminium chloride (Et_2AlCl), ethylaluminum sesquichloride (EASC), methylaluminoxane (MAO) and modified methylaluminoxane (MMAO), were explored at 30 ºC (entries 1 – 4, Table 2); the catalytic systems showed high activities in all cases. The polyethylenes obtained were measured by the gel permeation chromatography (GPC) and the differential scanning calorimetry (DSC), indicating the low molecular weight and narrow polydispersity as well as low melting point. The co-catalysts, being classified into aluminoxane and chloroaluminum; for which the highest activities were attained, MAO (entry 1, Table 2) and EASC (entry 4, Table 2), were selected for the further detailed exploration.

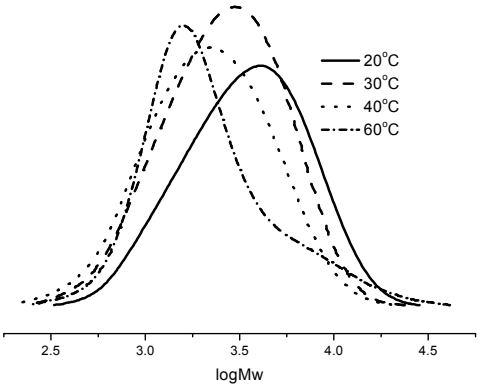

Figure 3. The GPC curves of polyethylenes depending reaction temperatures (entries 3, 6–8, Table 3)

Ethylene Polymerization Conducted with Ni1-Ni5/EASC systems. With the reaction temperature fixed at 30 ºC, the molar ratio Al/Ni (for EASC to complex **Ni3**) was changed from 600 to 1000 (entries 1 – 5, Table 3), and the highest activity of 4.39×10^6 g(PE)·mol^{-1}(Ni)·h^{-1} was achieved for the Al/Ni ratio of 800:1 (entry 3, Table 3). It was observed that the molecular weights of resulting polyethylenes decrease slightly along with the increasing molar ratios of aluminum to nickel; such behavior is commonly observed for the late transition metal complex pre-catalysts.[3,4] Interestingly, all polyethylenes

Dalton Transactions Accepted Manuscript

obtained showed the highly similar molecular weights and the narrow polydispersity, which probably indicate that the characteristic system could tailor polyethylenes for the unique molecular weights.

Fixing the Al/Ni ratio as 800:1, the reaction temperature was changed within the range from 20 to 60 °C (entries 3, 6 – 8, Table 3). As the catalytic activities decreased sharply along with the temperature elevated, the optimum temperature turned out to be 20 °C (entry 6, Table 3). Though the lower concentration of ethylene occurs at higher temperature,[18] such significant decrease in activities should respond to the deactivation of active species taking place at higher temperature, probably being decomposed along with generating Ni-hydride species.[12k] With the phenyl-fused pyridine frameworks, the better thermal stability was observed because of the stronger electron-donation to the nickel from the nitrogen of the pyridine, which stabilised the active species at higher temperature.[3e] Regarding the GPC curves of the resultant polyethylenes (shown in Figure 3), the higher temperature polymerization, the lower molecular weight of the resultant polyethylene; this is consistent with the fact that chain terminations is favored rather than chain propagation at the elevated temperature.[19]

Concerning the lifetime of active species, the polymerization was quenched within different periods (entries 6 and 10 – 12, Table 3). Though more polyethylenes were obtained along with prolonging the reaction time, the observing activities were gradually decreasing. Such catalytic behavior is similar to that of the nickel analogues,[13,15] moreover, ethylene polymerization proceeds without any induction period. All resultant polyethylenes show narrow polydispersity (1.64 – 1.73), which indicates the single site catalytic system. Surprisingly, the resultant polyethylenes possess molecular weights highly similar (entries 6 and 10 – 12, Table 3); probably the active species self-control in tailoring the resulting polyethylenes within the fixed range of molecular weights.

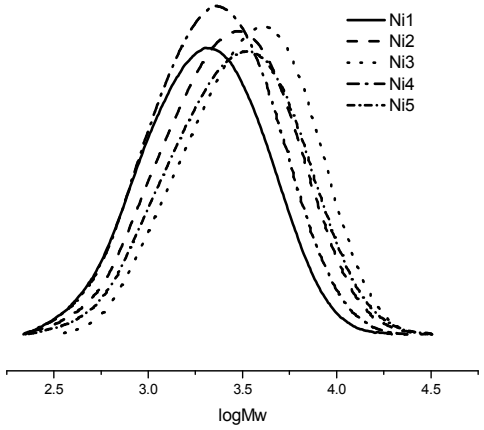

Figure 4. The GPC curves of polyethylene obtained by pre-catalysts (entries 6, 13–16, Table 3)

Table 2. Ethylene polymerization by **Ni3** with various co-catalysts [a]

Entry	Co-cat.	Al/Ni	*t* (min)	*T* (ºC)	Yield/g	Activity [b]	M_w[c]/g·mol^{-1}	M_w/M_n [c]	T_m/ºC [d]
1	MAO	2500	30	30	4.16	2.77	4045	1.69	57.2
2	MMAO	2500	30	30	2.17	1.45	4145	1.65	53.7
3	Et_2AlCl	400	30	30	1.93	1.29	3567	1.59	55.4
4	EASC	400	30	30	4.18	2.79	3206	1.69	46.1

[a] Conditions: 3 μmol of Ni; 10 atm of ethylene; total volume 100 mL. [b] 10^6 gPE·mol^{-1}(Ni)·h^{-1}. [c] Determined by gel permeation chromatography. [d] Determined by differential scanning calorimetry.

Table 3. Ethylene Polymerization by **Ni1–Ni5**/EASC [a]

Entry	Cat.	Al/Ni	*t* (min)	*T* (ºC)	Yield/g	Activity [b]	M_w[c]/g·mol^{-1}	M_w/M_n [c]	T_m/ºC [d]
1	**Ni3**	600	30	30	4.61	3.07	3397	1.59	44.1
2	**Ni3**	700	30	30	5.49	3.66	3374	1.68	41.4
3	**Ni3**	800	30	30	6.58	4.39	3342	1.68	41.2
4	**Ni3**	900	30	30	5.46	3.64	3238	1.64	40.4
5	**Ni3**	1000	30	30	3.49	2.33	3222	1.52	39.0
6	**Ni3**	800	30	20	7.07	4.71	4180	1.65	61.1
7	**Ni3**	800	30	40	3.40	2.27	2819	1.69	45.1
8	**Ni3**	800	30	60	0.75	0.50	2804	1.73	39.3
9[e]	**Ni3**	800	30	20	3.12	2.08	4061	1.67	45.1
10	**Ni3**	800	15	20	3.80	5.07	4088	1.64	60.2
11	**Ni3**	800	45	20	9.42	4.19	4217	1.73	58.6
12	**Ni3**	800	60	20	10.68	3.56	4269	1.73	60.3
13	**Ni1**	800	30	20	10.77	7.18	2453	1.62	58.0
14	**Ni2**	800	30	20	9.33	6.22	3481	1.84	56.0
15	**Ni4**	800	30	20	10.27	6.85	2825	1.68	56.5
16	**Ni5**	800	30	20	8.48	5.65	3830	1.79	56.9

[a] Conditions: 3 μmol of Ni; 30 min; 10 atm of ethylene; total volume 100 mL. [b] 10^6 gPE·mol^{-1}(Ni)·h^{-1}. [c] Determined by gel permeation chromatography. [d] Determined by differential scanning calorimetry. [e] 5 atm of ethylene.

Dalton Transactions Accepted Manuscript

This journal is © The Royal Society of Chemistry 20xx

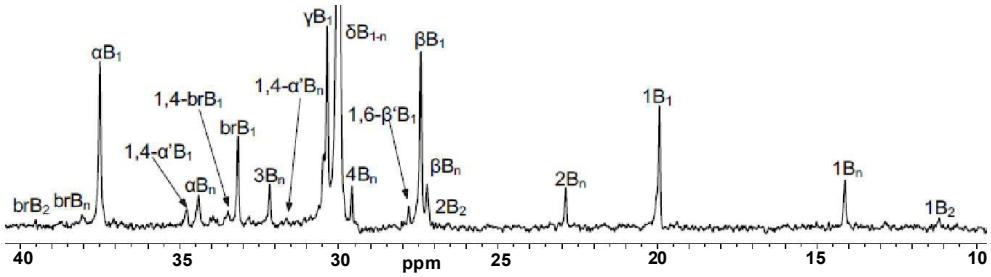

Figure 5. ^{13}C NMR spectrum of the polyethylene by Ni3/EASC at 20 °C (entry 6, Table 3). Guide for labels: For isolated branches, xBn, where n is the length of the branch and x is the carbon being discussed. The methyl group at the end of the branch numbered 1. Methylene in the backbone is labeled with Greek letters (such as α or β) which denote the carbon number which is away from a branch point. For paired branches, prefixes 1,m is used, where m is the number of carbons between two tertiary carbons, 1 being the first tertiary carbon and m the next.

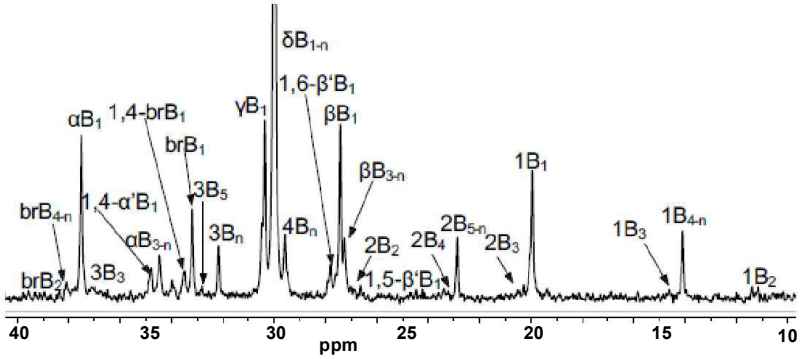

Figure 6. ^{13}C NMR spectrum of the polyethylene by Ni3/EASC at 60 °C (entry 8, Table 3)

Using the optimum conditions found for complex **Ni3**, all the complexes **Ni1 – Ni5** were examined (entries 6, 13 – 16, Table 3) to understand how the catalytic behavior is affected by the ligands used. In general, the GPC curves of all the polyethylenes obtained show narrow polydispersity, which indicate the behavior typical for the single site system (Figure 4). The polymerization activities decrease in the order **Ni1** [2,6-di(Me)] > **Ni2** [2,6-di(Et)] > **Ni3** [2,6-di(i-Pr)Me)], **Ni4** [2,4,6-tri(Me)] > **Ni5** [2,6-di(Et)-4-Me]. These results indicate that the bulky *ortho*-substituents (R^1 group, Scheme 2) of the phenyl group retard the coordination of ethylene onto the active sites; meanwhile the complexes **Ni4** and **Ni5** (entries 15 and 16, Table 3) indicated slightly lower activities than the corresponding analogous complexes **Ni1** and **Ni2** due to the existence of additional *para*-methyl of the phenyl within complexes **Ni4** and **Ni5**; the methyl substituent is an electron-donation, it was reported that the nickel cation with higher net charge brings about higher activities toward ethylene polymerization.[20]

The low molecular weights of obtained polyethylenes were confirmed by the low values of the melting points (T_m); however, the observing T_m values were very low and indicated the high possibility of branches within polyethylenes obtained. To assess the accurate numbers and kinds of the existing branches, the ^{13}C NMR measurements were conducted with the representative polyethylenes obtained with **Ni3**/EASC at 20 °C (entry 6, Table 3) and 60 °C (entry 8, Table 3). The NMR charts are shown in Figures 5 and 6, respectively; and their interpretations are collected in Table 4.[21] These samples are highly branched polyethylenes, with the branching density of 72 branches/1000 carbons in Figure 5 and 114 branches/1000 carbons in Figure 6. According to Figure 5, the majority of branches are methyl (64.5 %), and other branches included ethyl (5.5 %) as well as hexyl and longer branches (30.0 %) without propyl, butyl and amyl branches. In contrast, the higher number of branches is observed in Figure 6, there are propyl (4.3 %), butyl (9.3 %) and amyl (5.5 %) as well as methyl (54.0 %), ethyl (3.5 %) and

Table 4. Percentage of different branches from representative polyethylenes[21]

Sample / Branch	entry 6,Table 3		entry 8,Table 3		entry 5,Table 5	
	P_m[a]	P_t[b]	P_m[a]	P_t[b]	P_m[a]	P_t[b]
N_M(isolated)	6.9%	48.3%	4.29%	18.9%	5.9%	47.7%
$N_{M(1,4)}$	1.2%	8.4%	2.24%	9.8%	1.0%	8.4%
$N_{M(1,5)}$	0.0%	0.0%	2.99%	13.1%	0.0%	0.0%
$N_{M(1,6)}$	1.1%	7.7%	2.77%	12.2%	1.3%	10.2%
Total N_M	9.2%	64.5%	12.29%	54.0%	8.2%	66.3%
N_E	0.8%	5.5%	0.81%	3.5%	0.0%	0.0%
N_P	0.0%	0.0%	0.98%	4.3%	0.0%	0.0%
N_B	0.0%	0.0%	2.11%	9.3%	0.8%	6.9%
N_a	0.0%	0.0%	1.25%	5.5%	0.5%	4.0%
N_L(isolated)	4.1%	28.3%	5.31%	23.4%	2.8%	22.8%
$N_{L(1,4)}$	0.3%	1.7%	0.01%	0.0%	0.0%	0.0%
Total N_L	4.4%	30.0%	5.32%	23.4%	2.8%	22.8%
Total	14.4%	100.0%	22.8%	100.0%	12.3%	100.0%
CH_3/1000C	72		114		62	

[a] Percentage over main chain; [b] Percentage over total branches

Dalton Transactions Accepted Manuscript

hexyl and longer branches (23.4 %). Commonly, for higher numbers of branches, lower T_m values are observed.[13a,14b] The polyethylenes obtained with the title nickel systems are highly branched and formed due to the mechanism of the chain migration,[22] which is consistent to the observations performed by nickel complex pre-catalysts.[12,13,15]

Ethylene Polymerization by Systems Ni1-Ni5/MAO. Similarly, the catalytic systems activated with MAO were also investigated and the conditions were optimized for the complex **Ni3**. The Al/Ni molar ratio was changed from 2000 to 3500 at the temperature of 30 ºC (entries 1 – 4, Table 5) and the optimum ratio was observed for 2500 (entry 2, Table 5). Then the Al/Ni molar ratio was fixed at 2500 and the reaction temperature was screened between 20 to 60 ºC (entries 2, 5–7, Table 5) with the highest activity at 20 ºC. The activity decrease was observed along with the temperature elevated. The higher reaction temperature, the lower molecular weight of polyethylene obtained; which is consistent with the previous observation[23] as well as the results obtained herein for the above systems activated with EASC. The GPC curves shown in Figure 7 illustrate polyethylenes with lower molecular weight at the higher temperature, indicating chain termination favored at the elevated temperature. [19]

Under the optimum conditions, all the remaining nickel complexes were investigated in the ethylene polymerization (entries 5, 8 – 11, Table 5). Comparing with the systems activated by EASC, the correlation between the activities and the kind of substituents of the nickel complex pre-catalysts follows the same tendency as the order **Ni1**[2,6-di(Me)] > **Ni2** [2,6-di(Et)] > **Ni3** [2,6-di(i-Pr)Me)], and **Ni4** [2,4,6-tri(Me)] > **Ni5** [2,6-di(Et)-4-Me]; meanwhile, the bulkier the substituent (R^1) was used, the lower activity was observed, and the higher molecular weight polyethylene was obtained. The GPC curves of the polyethylenes obtained are shown in Figure 8. In general, the 9-aryliminocycloheptapyridylnickel complexes exhibited the comparable activities as did 8-arylimino-5,6,7-trihydroquinolylnickel analogues,[15] and higher activities than did the 2-iminopyridylnickel analogues.[13]

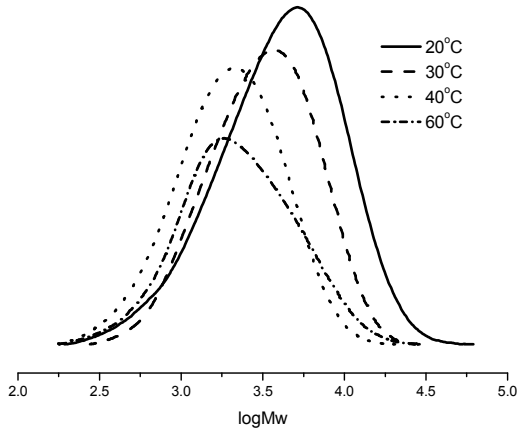

Figure 7. The GPC curves of polyethylene obtained at different temperatures (entries 2, 5-7, Table 5)

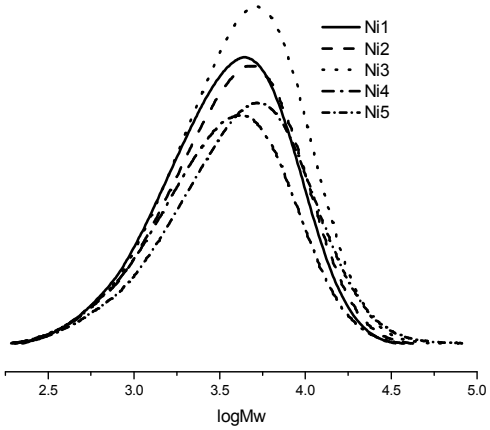

Figure 8. The GPC curves of polyethylene obtained by pre-catalysts (entries 5, 8-11, Table 5).

Table 5. Ethylene Polymerization by **Ni1**–**Ni5**/MAO [a]

Entry	Cat.	Al/Ni	t (min)	T (ºC)	Yield/g	Activity [b]	M_w [c]/g·mol^{-1}	M_w/M_n [c]	T_m/ºC [d]
1	**Ni3**	2000	30	30	1.11	0.74	3509	1.75	61.8
2	**Ni3**	2500	30	30	4.16	2.77	4045	1.69	57.2
3	**Ni3**	3000	30	30	3.95	2.63	4379	1.75	56.8
4	**Ni3**	3500	30	30	3.68	2.45	3775	1.76	56.8
5	**Ni3**	2500	30	20	5.31	3.54	5580	2.02	70.5
6	**Ni3**	2500	30	40	3.82	2.55	2539	1.68	54.1
7	**Ni3**	2500	30	60	0.95	0.63	2528	1.68	51.7
8	**Ni1**	2500	30	20	8.35	5.57	4779	1.92	77.7
9	**Ni2**	2500	30	20	7.98	5.32	5168	1.97	67.9
10	**Ni4**	2500	30	20	11.70	7.80	4535	1.99	64.7
11	**Ni5**	2500	30	20	9.02	6.01	5858	2.16	68.1

[a] Conditions: 3 µmol of Ni; 30 min; 10 atm of ethylene; total volume 100 mL. [b] 10^6 gPE·mol^{-1}(Ni)·h^{-1}. [c] Determined by gel permeation chromatography. [d] Determined by differential scanning calorimetry.

Dalton Transactions Accepted Manuscript

This journal is © The Royal Society of Chemistry 20xx

Please do not adjust margins

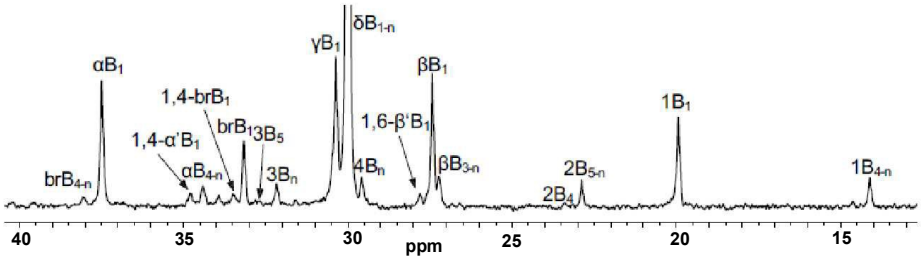

Figure 9 ^{13}C NMR spectrum of the polyethylene by Ni3/MAO at 20 °C (entry 5, Table 5)

The bulky substituent (R^1) probably hinders the ethylene coordination to the active species, but protects the active species in turn favoring the chain propagation toward polyethylene with higher molecular weight. The presence of the additional *para*-methyl substituent makes the significant difference in the activity. As shown in Table 3 in the systems with EASC, the complexes **Ni4** and **Ni5** bearing additional *para*-methyl substituent within the ligands show slightly lower activities than the analogous complexes **Ni1** and **Ni2** (entries 13 vs. 15, and 14 vs. 16, Table 3); in the systems with MAO, however, the complexes **Ni4** and **Ni5** exhibit significantly higher activities comparing with the analogous complexes **Ni1** and **Ni2** (entries 8 vs. 10, and 9 vs. 11, Table 5). These results indicate the characteristic features of co-catalysts applied; though the activation is generally considered as the alkylation occurred, MAO provides the alkylation along with the influence of electron-withdrawing alkoxyl group. Therefore, the system **Ni4**/MAO reaches the activity of up to 7.80 x 10^6 g of PE (mol of Ni)$^{-1}$ h^{-1}. According to the GPC curves (Figure 8), the polyethylenes obtained show the unimodal feature; this can be partly attributed to the single-site nature of the active species. The melting points (T_m) measured by DSC were relatively low, illustrating the presence of branched polyethylene. The polyethylene obtained with **Ni3**/MAO at 20 ºC (entry 5, Table 5) was characterized by ^{13}C NMR measurement and its spectrum is shown in Figure 9. Its interpretation according to literature[21] (see Table 4) indicates high branching density of 62 branches/1000 carbons including methyl (66.3 %), butyl (6.9 %) and amyl branches (4.0 %) as well as hexyl and longer branches (22.8 %).

All the title complexes exhibited the single-site nature and high catalytic activities toward ethylene polymerization. Upon activation with both EASC and MAO, the complex pre-catalysts generally show higher activities than nickel analogues bearing 8-arylimino-5,6,7-trihydroquinolines;[15] this is probably ascribed to the ring tension of fused-cycloheptance within the ligand framework. The resultant polyethylenes (PEs) were obtained with high number of branches and narrow polydispersity.

Conclusions

The 9-aryliminocycloheptapyridylnickel chloride complexes were synthesized and characterized. The molecular structures of nickel complexes were determined by single crystal X-ray diffraction and showed the dichloro-bridged dimer with the distorted square-pyramidal geometry around the nickel cation. Upon activation with either EASC or MAO, all title nickel complexes exhibited high activities toward ethylene polymerization. In comparison with nickel analogous pre-catalysts ligated by 2-iminopyridines[13] and 8-arylimino-5,6,7-trihydroquinolines,[15] the title pre-catalysts showed higher activities toward ethylene polymerization; though no clear evidence approves the source for the positive influence, the ring tension of fused-cycloheptance within the ligand framework is considered. The polyethylenes obtained had narrow polydispersity and low molecular weights, which indicates the possible applications as waxes, lubricants or addictives to pour-point depressants. These typical polyethylenes are potentially meeting some demand in industry, therefore further research of ligand modifications and optimization of catalytic conditions are still conducted in our group.

Experimental Section

General Considerations. All manipulations of air- and moisture-sensitive operations were carried out in a nitrogen atmosphere using standard Schlenk techniques. Toluene was refluxed over sodium and distilled under nitrogen prior to use. Methylaluminoxane (MAO, 1.46 M solution in toluene) and modified methylaluminoxane (MMAO, 1.93 M in *n*-heptane) were purchased from Akzo Nobel Corp. Ethylaluminium sesquichloride ($Et_3Al_2Cl_3$, EASC, 0.87 M in toluene) and diethylaluminium chloride (Et_2AlCl, 1.17 M in toluene) were purchased from Acros Chemicals. High-purity ethylene was purchased from Beijing Yanshan Petrochemical Co. and used as received. Other reagents were purchased from Beijing Chemical Reagents or AstaTech BioPharm. NMR spectra were recorded on Bruker DMX 400 MHz instrument at ambient temperature using TMS as an internal standard. IR spectra were detected on a Perkin-Elmer System 2000 FT-IR spectrometer. Elemental analysis was carried out using Flash EA 1112 microanalyzer. Molecular weights and molecular weight distribution (MWD) of polyethylenes were determined by the Agilent PL-GPC220 GPC/SEC High

Dalton Transactions Accepted Manuscript

Temperature System. The Columns are three 300×7.5mm PLgel 10um MIXED-B LS columns connected in series. The testing was undertaken at 150°C with the flow rate of 1.0ml/min. The eluent was 1, 2, 4-trichlorobenzene (TCB). Data collection and handling were carried out using Cirrus GPC Software and Multi Detector Software. The calibrants for constructing conventional calibration is Polystyrene Calibration Kit S-M-10from PL Company. The true average molecular weights of PE are transferred by inputting the M-H constants of PE. K of 0.727 and α of 40.6 are provided by PL Company. Samples were dissolved at a concentration of 0.5 to 2.5 mg/ml, depending on the molecular weights. DSC trace and melting points of polyethylene were obtained from the second scanning run on DSC Q2000 at a heating rate of 10 °C/min to 120 °C. ^{13}C NMR spectra of the polyethylenes were recorded on a Bruker DMX 300 MHz instrument at 135 °C in deuterated 1,2-dichlorobenzene using TMS as an internal standard.

Synthesis of 9-(2,6-dimethylphenylimino)-5,6,7,8-tetrahydrocyclohepta[*b*]pyridine (L1) : 9-(2,6-dimethyl-phenylamino)-5,6,7-trihydrocyclohepta[*b*]pyridine (L1'). A solution of 5,6,7,8-tetrahydrocyclohepta[b]pyridin-9-one (0.16 g, 1 mmol), 2,6-dimethylaniline (0.16 g, 1.2 mmol), and a catalytic amount of *p*-toluenesulfonic acid in chlorobenzene (20 mL) was refluxed for 6 h. The solvent was evaporated at reduced pressure, then the mixture was purified by silica gel column chromatography (petroleum ether/ethyl acetate = 25:1 v/v) to get the desired compound (yellow oil, L1: L1' = 1:0.21, 0.21 g, 75% yield). ^{1}H-NMR (400 MHz; $CDCl_3$; TMS): δ 8.65 (d, *J* = 4.4 Hz, 1H, L1-Py-H), 8.53 (d, *J* = 4.8 Hz, 1H, L1'-Py-H), 7.51 (d, *J* = 7.8 Hz, 1H, L1-Py-H), 7.26 (t, *J* = 4.4 Hz, 1H, L1-Ar-H), 7.15 (t, *J* = 4.8 Hz, 1H, L1'-Ar-H), 7.12 (d, *J* = 5.2, 2H, L1'-Ar-H), 7.05 (d, *J* = 7.6 Hz, 2H, L1-Ar-H), 6.92 (t, *J* = 7.8 Hz, 1H, L1-Py-H), 6.15 (s, 1H, L1'-NH), 4.56 (t, *J* = 6.8 Hz, 1H, L1'-CH-), 2.87 (t, *J* = 6.0 Hz, 2H, L1-CH_2-), 2.67 (t, *J* = 6.4 Hz, 2H, L1'-CH_2-), 2.35 (s, 6H, L1'-2 x CH_3), 2.31 (t, *J* = 6.0 Hz, 2H, L1-CH_2-), 2.16 (s, 6H, L1-2 x CH_3), 2.02 (m, 2H, L1'-CH_2-), 1.90 (m, 2H, L1'-CH_2-), 1.82 (m, 2H, L1-CH_2-), 1.62 (m, 2H, L1-CH_2-). ^{13}C NMR (100 MHz; $CDCl_3$; TMS): δ 172.8, 157.2, 148.4, 148.3, 137.1, 135.2, 134.7, 128.3, 128.0, 125.0, 123.9, 122.8, 122.1, 31.7, 31.6, 25.8, 23.4, 18.3, 18.1. FT-IR (KBr, cm^{-1}): 3358.5(ν_{N-H}, w), 2929.6(s), 2856.1(m), 2361.1(w), 2024.9(w), 1981.4(w), 1733.2(m), 1640.3($\nu_{C=N}$, s), 1592.2(m), 1567.3(m), 1435.2(vs), 1374.3(w), 1243.0(m), 1196.8(s), 1093.5(s), 1041.7(m), 964.6(w), 857.1(w), 794.5(m), 764.7(s), 718.9(w). Anal. Calcd for $C_{18}H_{20}N_2$ (264.4): C, 81.78; H, 7.63; N, 10.60; Found: C, 81.90; H, 7.89; N, 10.50.

Synthesis of 9-(2,6-diethylphenylimino)-5,6,7,8-tetrahydrocyclohepta[*b*]pyridine (L2) : 9-(2,6-diethyl-phenylamino)-5,6,7-trihydrocyclohepta[*b*]pyridine (L2'). Using the same procedure as for the synthesis of L1, we got L2 and L2' (yellow oil, L2: L2' = 1:0.23, 74% yield). ^{1}H-NMR (400 MHz; $CDCl_3$; TMS): δ 8.65 (d, *J* = 4.4 Hz, 1H, L2-Py-H), 8.53 (d, *J* = 3.6 Hz, 1H, L2'-Py-H), 7.52 (d, *J* = 7.8 Hz, 1H, L2-Py-H), 7.35 (d, *J* = 7.8 Hz, 1H, L2'-Py-H), 7.26 (t, *J* = 4.8 Hz, 1H, L2-Ar-H), 7.15 (t, *J* = 4.4 Hz, 1H, L2'-Ar-H), 7.12 (d, *J* = 8.4 Hz, 2H, L2-Ar-H), 7.03 (t, *J* = 7.6 Hz, 1H, L2-Py-H), 6.20 (s, 1H, L2'-NH), 4.56 (t, *J* = 6.8 Hz, 1H, L2'-CH-), 2.86 (t, *J* = 6.0 Hz, 2H, L2-CH_2-), 2.73 (m, 4H, L2'-2 x Ar-CH_2-), 2.67 (t, *J* = 6.4 Hz, 2H, L2'-CH_2-), 2.57 (m, 2H, L2-Ar-CH_2-), 2.41 (m, 2H, L2-Ar-CH_2-), 2.30 (t, *J* = 6.0 Hz, 2H, L2-CH_2-), 2.00 (m, 2H, L2'-CH_2-), 1.90 (m, 2H, L2'-CH_2-), 1.81 (m, 2H, L2-CH_2-), 1.60 (m, 2H, L2-CH_2-), 1.25-1.23 (m, 6H, 2 x CH_3). ^{13}C NMR (100 MHz; $CDCl_3$; TMS): δ 172.7, 157.1, 148.4, 147.4, 146.6, 137.0, 134.6, 130.7, 126.3, 125.6, 123.9, 123.2, 31.7, 31.6, 25.7, 24.5, 24.1, 22.9, 15.0, 13.7. FT-IR (KBr, cm^{-1}): 3360.0(ν_{N-H}, w), 2961.1(m), 2929.7(s), 2865.5(m), 1637.6($\nu_{C=N}$, s), 1591.2(w), 1566.2(m), 1446.6(vs), 1372.0(w), 1327.7(w), 1264.2(w), 1189.7(m), 1102.8(m), 1043.5(w), 963.6(w), 862.0(w), 794.0(m), 764.6(s), 722.8(w). Anal. Calcd for $C_{20}H_{24}N_2$ (292.4): C, 82.15; H, 8.27; N, 9.58; Found: C, 81.93; H, 8.33; N, 9.68.

Synthesis of 9-(2,6-diisopropylphenylimino)-5,6,7,8-tetrahydrocyclohepta[*b*]pyridine (L3) : 9-(2,6-diisopropyl-phenylamino)-5,6,7-trihydrocyclohepta[*b*]pyridine (L3'). Using the same procedure as for the synthesis of L1, we got L3 and L3' (yellow oil, L3: L3' = 1:0.09, 83% yield). ^{1}H-NMR (400 MHz; $CDCl_3$; TMS): δ 8.66 (d, *J* = 4.4 Hz, 1H, L3-Py-H), 8.54 (d, *J* = 4.4 Hz, 1H, L3'-Py-H), 7.51 (d, *J* = 7.8 Hz, 1H, L3-Py-H), 7.34 (d, *J* = 6,8 Hz, 1H, L3'-Py-H), 7.26 (t, *J* = 4.8 Hz, 1H, L3-Ar-H), 7.16 (d, *J* = 6.8 Hz, 2H, L3-Ar-H), 7.07 (t, *J* = 7.8 Hz, 1H, L3-Py-H), 6.15 (s, 1H, L3'-NH), 4.55 (t, *J* = 6.8 Hz, 1H, L3'-CH-), 3.39 (m, 4H, L3'-2 x Ar-CH-), 2.98 (m, 2H, L3-Ar-CH-), 2.86 (t, *J* = 6.4 Hz, 2H, L3-CH_2-), 2.67 (t, *J* = 6.4 Hz, 2H, L3'-CH_2-), 2.34 (t, *J* = 6.0 Hz, 2H, L3-CH_2-), 1.99 (m, 2H, L3'-CH_2-), 1.92 (m, 2H, L3'-CH_2-), 1.80 (m, 2H, L3-CH_2-), 1.61 (m, 2H, L3-CH_2-), 1.27-1.17 (m, 12H, 4 x CH_3). ^{13}C NMR (100 MHz; $CDCl_3$; TMS): δ 173.1, 157.0, 148.6, 146.0, 137.0, 135.9, 134.5, 124.0, 123.7, 123.3, 60.5, 31.9, 31.4, 28.0, 25.8, 24.2, 23.2, 22.5, 14.3. FT-IR (KBr, cm^{-1}): 3364.0(ν_{N-H}, w), 3056.4(w), 2957.8(s), 2929.3(s), 2864.4(m), 1635.2($\nu_{C=N}$, m), 1566.5(m), 1438.3(vs), 1380.9(w), 1360.4(w), 1325.9(w), 1298.5(w), 1256.9(m), 1183.5(w), 1142.9(w), 1102.8(m), 1048.6(w), 962.4(w), 933.8(w), 908.3(w), 856.7(w), 794.1(m), 763.9(s). Anal. Calcd for $C_{22}H_{28}N_2$ (320.5): C, 82.45; H, 8.81; N, 8.74; Found: C, 82.09; H, 8.74; N, 8.80.

Synthesis of 9-mesitylimino-5,6,7,8-tetrahydrocyclohepta[*b*]pyridine (L4) : 9-mesitylamino-5,6,7-trihydrocyclohepta[*b*]pyridine (L4'). Using the same procedure as for the synthesis of L1, we got L4 and L4' (yellow oil, L4: L4' = 1:0.68, 81% yield). ^{1}H-NMR (400 MHz; $CDCl_3$; TMS): δ 8.66 (d, *J* = 4.8 Hz, 1H, L4-Py-H), 8.53 (d, *J* = 4.8 Hz, 1H, L4'-Py-H), 7.53 (d, *J* = 6.8 Hz, 1H, L4-Py-H), 7.46 (d, *J* = 6.0 Hz, 1H, L4'-Py-H), 7.28 (t, *J* = 4.4 Hz, 1H, L4-Py-H), 7.16 (t, *J* = 4.8 Hz, 1H, L4'-Py-H), 6.96 (s, *2*H, L4'-Ar-H), 6.90 (s, *2*H, L4-Ar-H), 6.06 (s, 1H, L4'-NH), 4.59 (t, *J* = 6.8 Hz, 1H, L4'-CH-), 2.88 (t, *J* = 6.4 Hz, 2H, L4-CH_2-), 2.69 (t, *J* = 6.8 Hz, 2H, L4'-CH_2-), 2.35-2.31 (m, 9H, L4-3 x CH_3), 2.15 (s, 9H, L4'-3 x CH_3), 2.06 (m, 2H, L4'-CH_2-), 1.93 (m, 2H, L4-CH_2-), 1.84 (m, 2H, L4-CH_2-), 1.64 (m, 2H, L4-CH_2-). ^{13}C NMR (100 MHz; $CDCl_3$; TMS): δ 173.1, 157.3, 148.3, 146.7, 145.9, 141.0, 137.1, 137.0, 136.9, 135.1, 134.6, 132.0, 129.0, 128.7, 124.8, 123.9, 122.1, 99.3, 53.5, 32.9, 32.1, 31.8, 31.5, 25.8, 24.0, 23.4, 20.9, 20.8, 18.1, 18.0. FT-IR (KBr, cm^{-1}): 3360.6(ν_{N-H}, w), 2927.2(s), 2855.1(m), 1736.6(m), 1637.4($\nu_{C=N}$, s), 1566.2(m), 1478.5(s), 1434.2(vs), 1373.5(w), 1243.3(m),

Dalton Transactions Accepted Manuscript

This journal is © The Royal Society of Chemistry 20xx

1208.0(m), 1145.5(w), 1098.5(w), 1038.0(m), 958.8(w), 852.7(w), 798.5(s), 749.8(m), 713.7(w). Anal. Calcd for $C_{19}H_{22}N_2$ (278.4): C, 81.97; H, 7.97; N, 10.06; Found: C, 81.81; H, 8.05; N, 10.12.

Synthesis of 9-(2,6-diethyl-4-methylphenylimino)-5,6,7,8-tetrahydrocyclohepta[*b*]pyridine (L5) : 9-(2,6-diethyl-4-methylphenylamino)-5,6,7-trihydrocyclohepta[*b*]pyridine (L5'). Using the same procedure as for the synthesis of L1, we got L5 and L5' (yellow oil, L5: L5' = 1:0.30, 81% yield). ^{1}H-NMR (400 MHz; $CDCl_3$; TMS): δ 8.67 (d, *J* = 4.8 Hz, 1H, L5-Py-H), 8.56 (d, *J* = 4.8 Hz, 1H, L5'-Py-H), 7.54 (t, *J* = 6.4 Hz, 1H, L5-Py-H), 7.46 (t, *J* = 6.4 Hz, 1H, L5'-Py-H), 7.28 (d, *J* = 4.8 Hz, 1H, L5-Py-H), 7.22 (d, *J* = 4.8 Hz, 1H, L5'-Py-H), 7.00 (s, 2H, L5'-Ar-H), 6.96 (s, 2H, L5-Ar-H), 6.10 (s, 1H, L5'-NH), 4.57 (t, *J* = 6.8 Hz, 1H, L5'-CH-), 2.88 (t, *J* = 6.4 Hz, 2H, L5-CH_2-), 2.70 (m, 2H, L5-CH_2-), 2.59 (m, 2H, L5-Ar-CH_2-), 2.41(m, 2H, L5-Ar-CH_2-), 2.37 (s, 3H, L5'-CH_3), 2.36 (s, 3H, L5-CH_3), 2.33 (m, 2H, L5'-CH_2-), 2.02 (m, 2H, L5'-CH_2-), 1.91 (m, 2H, L5'-CH_2-), 1.82 (m, 2H, L5-CH_2-), 1.62 (m, 2H, L5-CH_2-), 1.26-1.21 (m, 6H, L5'-2 x CH_3). ^{13}C NMR (100 MHz; $CDCl_3$; TMS): δ 173.1, 157.3, 148.4, 146.7, 145.0, 141.7, 137.0, 134.6, 132.3, 130.7, 127.8, 127.2, 126.5, 123.9, 122.1, 99.4, 53.5, 31.7, 31.6, 25.8, 24.6, 24.1, 23.0, 21.2, 15.2, 13.9. FT-IR (KBr, cm^{-1}): 3363.0(ν_{N-H}, w), 2961.4(m), 2929.4(s), 2862.8(m), 1737.5(m), 1637.1($\nu_{C=N}$, s), 1566.4(m), 1477.6(vs), 1435.3(s), 1371.7(w), 1241.7(m), 1204.4(w), 1143.7(w), 1081.6(w), 1039.5(m), 964.5(w), 857.0(m), 795.4(s), 753.6(m), 657.1(w). Anal. Calcd for $C_{21}H_{26}N_2$ (306.4): C, 82.31; H, 8.55; N, 9.14; Found: C, 82.01; H, 8.45; N, 9.11.

Synthesis of 9-(2,6-dimethylphenylimino)-5,6,7,8-tetrahydrocyclohepta[*b*]pyridylnickel(II) dichloride (Ni1). A solution of $NiCl_2{\cdot}6H_2O$ (2 mmol) in ethanol was added dropwise to the corresponding ligand (2 mmol) in ethanol/ dichloromethane. The mixture was stirred at room temperature overnight, then the precipitate was collected by filtration and washed with diethyl ether (3 x 5 mL), then dried under vacuum, we got Ni1 (yellow powder, 78 % yield). FT-IR (KBr, cm^{-1}): 2932.5(m), 2863.7(m), 2160.7(w), 2025.3(w), 1980.3(w), 1608.8($\nu_{C=N}$, m), 1573.5(s), 1447.7(s), 1336.7(w), 1270.7(m), 1199.6(s), 1112.7(m), 979.0(w), 871.6(w), 777.5(m). Anal. Calcd for $C_{21}H_{26}Cl_2N_2Ni$ (394): C, 54.88; H, 5.12; N, 7.11; Found: C, 54.60; H, 5.16; N, 7.14.

Synthesis of 9-(2,6-diethylphenylimino)-5,6,7,8-tetrahydrocyclohepta[*b*]pyridylnickel(II) dichloride (Ni2). Using the similar procedure as for the synthesis of Ni1, we got Ni2 (yellow powder, 87 % yield). FT-IR (KBr, cm^{-1}): 2964.1(m), 2929.4(m), 2866.2(m), 2166.3(w), 1975.4(w), 1608.2($\nu_{C=N}$, s), 1573.8(s), 1453.4(vs), 1338.6(w), 1273.2(m), 1248.3(w), 1196.5(s), 1118.2(m), 1062.3(w), 973.0(w), 872.1(w), 806.1(s), 775.1(m), 719.6(w). Anal. Calcd for $C_{20}H_{24}Cl_2N_2Ni$ (422): C, 56.92; H, 5.73; N, 6.64; Found: C, 56.81; H, 5.70; N, 6.32.

Synthesis of 9-(2,6-diisopropylphenylimino)-5,6,7,8-tetrahydrocyclohepta[*b*]pyridylnickel(II) dichloride (Ni3). Using the similar procedure, we got Ni3 (light green powder, 93 % yield). FT-IR (KBr, cm^{-1}): 2965.4(m), 2929.8(m), 2866.2(m), 2183.0(w), 2017.5(w), 1607.2($\nu_{C=N}$, m), 1575.7(s), 1456.5(s), 1382.7(w), 1323.5(w), 1270.8(w), 1179.2(m), 1116.0(m), 1081.5(m), 1046.8(s), 976.8(w), 880.5(w), 823.1(m), 793.4(m), 766.0(s), 721.2(m). Anal. Calcd for $C_{22}H_{28}Cl_2N_2Ni$ (450.1): C, 58.71; H, 6.27; N, 6.22; Found: C, 58.75; H, 6.35; N, 6.17.

Synthesis of 9-mesitylimino-5,6,7,8-tetrahydrocyclohepta-[*b*]pyridylnickel(II) dichloride (Ni4). Using the similar procedure, we got Ni4 (yellow powder, 86 % yield). FT-IR (KBr, cm^{-1}): 2923.9(m), 2858.9(m), 2161.1(w), 1974.2(w), 1612.9($\nu_{C=N}$, s), 1574.3(s), 1446.4(vs), 1379.8(w), 1338.0(w), 1273.5(m), 1209.8(s), 1155.9(m), 1113.0(m), 1083.2(w), 976.7(w),919.8(w), 855.7(m), 812.7(s), 722.2(m). Anal. Calcd for $C_{19}H_{22}Cl_2N_2Ni$ (408): C, 55.93; H, 5.44; N, 6.87; Found: C, 55.70; H, 5.28; N, 6.61.

Synthesis of 9-(2,6-diethyl-4-methylphenylimino)-5,6,7,8-tetrahydrocyclohepta[*b*]pyridylnickel(II) dichloride (Ni5). Using the similar procedure, we got Ni5 (yellow powder, 89 % yield). FT-IR (KBr, cm^{-1}): 2930.7(m), 2867.6(m), 2160.7(w), 2025.0(w), 1610.4($\nu_{C=N}$, s), 1573.8(s), 1453.9(vs), 1376.9(w), 1337.6(m), 1272.4(m), 1205.6(m), 1155.1(m), 1113.9(m), 976.6(w), 923.6(w), 858.8(s), 809.2(s), 718.9(m). Anal. Calcd for $C_{21}H_{26}Cl_2N_2Ni$ (436): C, 57.84; H, 6.01; N, 6.42; Found: C, 57.77; H, 5.90; N, 6.54.

Procedure for Ethylene Polymerization. Ethylene polymerization was carried out in a stainless steel autoclave (250 mL capacity) equipped with an ethylene pressure control system, a mechanical stirrer and a temperature controller. The autoclave was vacuumized and filled with ethylene for three times. When the desired reaction temperature was reached, under ethylene atmosphere, toluene, co-catalyst (MAO, MMAO, EASC Et_2AlCl), and a toluene solution of the catalytic precursor (the total volume was 100 mL) were injected into the autoclave by using syringes, and then the ethylene pressure was increased to the desired value, and maintained at this level with constant feeding of ethylene. After given time, the reactor was cooled with ice-water bath and the excess ethylene was vented. The resultant mixture was poured into 10% HCl/ethanol solution, and the polymer was collected and washed with ethanol several times and dried *in vacuo*.

X-ray Crystallographic Studies. Single crystals of the nickel complexes **Ni1** and **Ni3** suitable for X-ray diffraction analysis were obtained by slow diffusion of diethyl ether into the corresponding dichloromethane solutions under nitrogen atmosphere at room temperature. Data collection for them were carried out on Rigaku Saturn 724 + CCD diffractometer with graphite-monochromated Mo Kα radiation (λ = 0.71073 Å). Cell parameters were obtained by global refinement of the positions of all collected reflections. Intensities were corrected for Lorentz and polarization effects and empirical absorption. The structures were solved by direct methods, and refined by full-matrix least squares on F^2. All hydrogen atoms were placed in calculated positions. Structure refinement were performed by using the SHELXL-97 package.[24] The SQUEEZE option of the crystallographic program PLATON[25] was used to remove free solvents from the structures of **Ni1** and **Ni3**. Details of the X-ray structure determinations and refinements are provided in Table 6.

Dalton Transactions Accepted Manuscript

Table 6. Crystal data and Structure Refinement for **Ni1** and **Ni3**.

	Ni1	**Ni3**
Crystal colour	Red	Yellow
Empirical formula	$C_{36}H_{40}N_4Cl_4Ni_2$	$C_{44}H_{56}N_4Cl_4Ni_2$
Formula weight	787.94	900.15
T (K)	173 (2)	173 (2)
wavelength (Å)	0.71073	0.71073
cryst syst	Monoclinic	Monoclinic
space group	P2(1)/c	P2(1)/n
a (Å)	15.376(3)	10.330(2)
b (Å)	10.184(2)	14.356(3)
c (Å)	22.865(5)	14.999(3)
α (°)	90	90
β (°)	102.27(3)	104.47(3)
γ (°)	90	90
V (Å^3)	3498.9(12)	2153.8(8)
Z	4	2
Dcalcd. (mgm^{-3})	1.496	1.388
μ (mm^{-1})	1.158	1.158
F(000)	1632	944
Cryst size (mm)	0.64×0.40×0.26	0.64×0.59×0.17
θ range (°)	1.36 - 27.52	1.99 – 27.50
limiting indices	-19 ≤ h ≤ 19 -13 ≤ k ≤ 12 -29 ≤ l ≤ 29	-7 ≤ h ≤ 13 -18 ≤ k ≤ 18 -19 ≤ l ≤ 19
no. of rflns collected	24004	11130
no. unique rflns [R(int)]	7980(0.0415)	4924(0.0248)
completeness to ϑ (%)	99.2	99.5
Goodness of fit on F^2	1.123	1.132
Final R indices [I > 2σ(I)]	R1 = 0.0447 wR2 = 0.1083	R1 = 0.0449 wR2 = 0.1303
R indices (all data)	R1 = 0.0488 wR2 = 0.1128	R1 = 0.0501 wR2 = 0.1385
largest diff peak and hole (e Å^{-3})	0.417 and -0.878	0.631 and -0.795

Acknowledgements

This work is supported by National Natural Science Foundation of China (NSFC Nos. 21374123, 21473160 and U1362204).

References

1 (a) L. K. Johnson, C. M. Killian and M. Brookhart, *J. Am. Chem. Soc.*, 1995, **117**, 6414; (b) C. M. Killian, D. J. Tempel, L. K. Johnson and M. Brookhart, *J. Am. Chem. Soc.*, 1996, **118**, 11664.

2 (a) B. L. Small, M. Brookhart and A. M. A. Bennett, *J. Am. Chem. Soc.*, 1998, **120**, 4049; (b) G. J. P. Britovsek, V. C. Gibson, B. S. Kimberley, P. J. Maddox, S. J. McTavish, G. A. Solan, A. J. P. White and D. J. Williams, *Chem. Commun.*, 1998, 849.

3 (a) S. Wang, W.-H. Sun and C. Redshaw, *J. Organomet. Chem.*, 2014, **751**, 717; (b) R. Gao, W.-H. Sun and C. Redshaw, *Catal. Sci. Technol.*, 2013, **3**, 1172; (c) C. Bianchini, G. Giambastiani, L. Luconi and A. Meli, *Coord. Chem. Rev.*, 2010, **254**, 431; (d) F. Speiser, P. Braunstein and L. Saussine, *Acc. Chem. Res.*, 2005, **38**, 784; (e) S. Song, T. Xiao, L. Wang, C. Redshaw, F. Wang and W.-H. Sun, *J. Organomet. Chem*. 2012, **699**, 18.

4 (a) J. Ma, C. Feng, S. Wang, K.-Q. Zhao, W.-H. Sun, C. Redshaw and G. A. Solan, *Inorg. Chem. Front.*, 2014, **1**, 14; (b) W. Zhang, W.-H. Sun and C. Redshaw, *Dalton Trans.*, 2013, **42**, 8988; (c) V. C. Gibson, C. Redshaw and G. A. Solan, *Chem. Rev.*, 2007, **107**, 1745; (d) W. -H. Sun, W. Zhao, J. Yu, W. Zhang, X. Hao and C. Redshaw, *Macromol. Chem. Phys.*, 2012, **213**, 1266; (e) Q. Xing, T. Zhao, Y. Qiao, L. Wang, C. Redshaw and W. -H. Sun, *RSC Adv.*, 2013, **3**, 26184; (f) Q. Xing, T. Zhao, S. Du, W. Yang, T. Liang, C. Redshaw and W. -H. Sun, *Organometallics*, 2014, **33**, 1382.

5 (a) W.-H. Sun, S. Jie, S. Zhang, W. Zhang, Y. Song, H. Ma, J. Chen, K. Wedeking and R. Fröhlich, *Organometallics*, 2006, **25**, 666; (b) S. Jie, S. Zhang, W.-H. Sun, X. Kuang, T. Liu and J. Guo, *J. Mol. Catal. A: Chem.*, 2007, **269**, 85; (c) M. Zhang, W. Zhang, T. Xiao, J.-F. Xiang, X. Hao and W.-H. Sun, *J. Mol. Catal. A: Chem.*, 2010, **320**, 92; (d) W.-H. Sun, S. Jie and S. Zhang, CN Pat. Appl. ZL200510066427.2 (2005); (e) W.-H. Sun, M. Zhang and W. Zhang, CN Pat. Appl. ZL200910236804.0 (2009).

6 (a) J. Yu, H. Liu, W. Zhang, X. Hao and W.-H. Sun, *Chem. Commun.*, 2011, **47**, 3257; (b) J. Lai, W. Zhao, W. Yang, C. Redshaw, T. Liang, Y. Liu and W. -H. Sun, P*olym. Chem.*, 2012, **3**, 787; (c) W. Zhang, W. B. Chai, W. -H. Sun, X. Q. Hu and C. Redshaw *Organometallics*, 2012, **31**, 5039; (d) S. Wang, W. Zhao, X. Hao, B. Li, C. Redshaw, Y. Li and W.-H. Sun, *J. Organomet. Chem.*, 2013, **731**, 78.

7 (a) P. J. Shapiro, E. Bunel, W. P. Schaefer and J. E. Bercaw, *Organometallics*, 1990, **9**, 867; (b) J. C. Stevens, F. J. Timmers, D. R. Wilson, G. F. Schmidt, P. N. Nickias, R. K. Rosen, G. W. McKnight and S. Lai, Eur. Pat. Appl. 0416815A2 (1991); (c) P. J. Shapiro, W. D. Cotter, W. P. Schaefer, J. A. Labinger and J. E. Bercaw, *J. Am. Chem. Soc.*, 1994, **116**, 4623.

8 (a) W. Keim, A. Behr, B. Limbäcker and C. Krüger, *Angew. Chem., Int. Ed. Engl.,* 1983, **22,** 503; (b) W. Keim, A. Behr and G. Kraus, *J. Organomet. Chem.*, 1983, **251**, 377.

9 (a) W.-H. Sun, Z. Li, H. Hu, B. Wu, H. Yang, N. Zhu, X. Leng and H. Wang, *New J. Chem.*, 2002, **26**, 1474; (b) H.-P. Chen, Y.-H. Liu, S.-M. Peng and S.-T. Liu, *Organometallics*, 2003, **22**, 4893; (c) J. Hou, W.-H. Sun, S. Zhang, H. Ma, Y. Deng and X. Lu, *Organometallics*, 2006, **25**, 236; (d) J. Flapper, H. Kooijman, M. Lutz, A. L. Spek, P. W. N. Van Leeuwen, C. J. Elsevier and P. C. J. Kamer, *Organometallics*, 2009, **28**, 3272.

10 (a) C. Wang, S. Friedrich, T. R. Younkin, R. T. Li, R. H. Grubbs, D. A. Bansleben and M. W. Day, *Organometallics*, 1998, **17**, 3149; (b) T. R. Younkin, E. F. Connor, J. I. Henderson, S. K. Friedrich, R. H. Grubbs and D. A. Bansleben, *Science*, 2000, **287**, 460; (c) L. Wang, W.-H. Sun, L. Han, Z. Li, Y. Hu, C. He and C. Yan, *J. Organomet. Chem.*, 2002, **650**, 59; (d) Q.-S. Shi, X. Hao, C. Redshaw and W.-H. Sun, *Chinese J. Polym. Sci.*, 2013, **31**, 769; (e) W.-H. Sun, W. Zhang, T. Gao, X. Tang,

Dalton Transactions Accepted Manuscript

This journal is © The Royal Society of Chemistry 20xx

L. Chen, Y. Li and X. Jin, *J. Organomet. Chem.*, 2004, **689**, 917.

11 (a) S. Benson, B. Payne and R. M. Waymouth, *J. Polym. Sci., Part A: Polym. Chem.*, 2007, **45**, 3637; (b) S. O. Ojwach, I. A. Guzei, L. L. Benade, S. F. Mapolie and J. Darkwa, *Organometallics*, 2009, **28**, 2127; (c) P. Hao, S. Song, T. Xiao, Y. Li, C. Redshaw and W.-H. Sun, *Polyhedron,* 2013, **52**, 1138; (d) F. He, X. Hao, X. Cao, C. Redshaw and W.-H. Sun, *J. Organomet. Chem.,* 2012, **712**, 46; (e) L. Zhang, X. Hou, J. Yu, X. Chen, X. Hao and W.-H. Sun, *Inorg. Chim. Acta,* 2011, **379**, 70 ; (f) X. Chen, L. Zhang, J. Yu, X. Hao, H. Liu and W.-H. Sun, *Inorg. Chim. Acta,* 2011, **370**, 156; (g) H. Liu, L. Zhang, L. Chen, C. Redshaw, Y.Li and W.-H. Sun, *Dalton Trans.,* 2011, **40**, 2614; (h) X. Chen, L. Zhang, T. Liang, X. Hao and W.-H. Sun, *C. R. Chim.*, 2010, **13**, 1450; (i) C. Obuah, B. Omondi, K. Nozaki and J. Darkwa, *J. Mol. Catal. A: Chem.,* 2014, **382**, 31.

12 (a) Q. Liu, W. Zhang, D. Jia, X. Hao, C. Redshaw and W.-H. Sun, *Appl. Catal. A: Gen.*, 2014, **475**, 195; (b) D. Meinhard, P. Reuter and B. Pieger, *Organometallics*, 2007, **26**, 751; (c) H. Zou, F. M. Zhu, Q. Wu, J. Y. Ai and S. A. Lin, *J. Polym. Sci., Part A: Polym. Chem.*, 2005, **43**, 1325; (d) M. Helldorfer, J. Backhus, W. Milius and H. G. Alt, *J. Mol. Catal. A: Chem.*, 2003, **193**, 59; (e) M. Schmid, R. Eberhardt, M. Klinga, M. Leskela and B. Rieger, *Organometallics*, 2001, **20**, 2321; (f) P. D. Gates, S. A. Svejda, E. C. Onate, M. Killian, L. K. Johnson, P. S. White and M. Brookhart, *Macromolecules*, 2000, **33**, 2320; (g) H. Liu, W. Zhao, X. Hao, C. Redshaw, W. Huang and W.-H. Sun, *Organometallics*, 2011, **30**, 2418; (h) H. Liu, W. Zhao, J. Yu, W. Yang, X. Hao, C. Redshaw, L. Chen and W.-H. Sun, *Catal. Sci. Technol.*, 2012, **2**, 415; (i) S. Kong, C.-Y. Guo, W. Yang, L. Wang, W.-H. Sun and R. Glaser, *J. Organomet. Chem.*, 2013, **725**, 37; (j) C. Wen, S. Yuan, Q. Shi, E. Yue, D. Liu and W.-H. Sun, *Organometallics*, 2014, **33**, 7223; (k) D. H. Camacho, E. V. Salo, J. W. Ziller and Z. Guan, *Angew. Chem. Int. Ed.*, 2004, **43**, 1821.

13 (a) D. P. Gates, S. A. Svejda, E. Onate, C. M. Killian, L. K. Johnson, P. S. White and M. Brookhart, *Macromolecules*, 2000, **33**, 2320; (b) E. Yue, L. Zhang, Q. Xing, X. Cao, X. Hao, C. Redshaw and W. -H. Sun, *Dalton Trans.*, 2014, **43**, 423; (c) E. Yue, L. Zhang, Q. Xing, L. Wang, C. Redshaw and W. -H. Sun, *Dalton Trans.*, 2014, **43**, 3339; (d) W.-H. Sun, S. Song, B. Li, C. Redshaw, X. Hao, Y. Li and F. Wang, *Dalton Trans.*, 2012, **41**, 11999; (e) J. M. Benito, E. Jesus, F. J. Mata, J. C. Flores, R. Gomez and P. Gomez-Sal, *Organometallics*, 2006, **25**, 3876; (f) T. V. Laine, U. Piironen, K. Lappalainen, M. Klinga, E. Aitola and M. Leskela, *J. Organomet. Chem.*, 2000, **606**, 112; (g) T. V. Laine, K. Lappalainen, J. Liimatta, E. Aitola, B. Lofgren and M. Leskela, *Macromol. Rapid Commun.*, 1999, **20**, 487 ; (h) T. V. Laine, M. Klinga and M. Leskela, *Eur. J. Inorg. Chem.*, 1999, 959; (i) S. Jie, D.Zhang, T. Zhang, W. -H. Sun, J. Chen, Q. Ren, D. Liu, G. Zheng and W. Chen, *J. Organomet. Chem.*, 2005, **690**, 1739; (j) B. K. Bahuleyan, U. Lee, C.-S. Ha and I. Kim, *Appl. Catal., A*, 2008, **351**, 36; (k) J. D. A. Pelletier, J. Fawcett, K. Singh and G. A. Solan, *J. Organomet. Chem.*, 2008, **693**, 2723.

14 (a) J. Yu, X. Hu, Y. Zeng, L. Zhang, C. Ni, X. Hao and W.-H. Sun, *New J. Chem.*, 2011, **35**, 178; (b) W. Chai, J. Yu, L. Wang, X. Hu, C. Redshaw and W.-H. Sun, *Inorg. Chim. Acta.*, 2012, **385**, 21.

15 (a) J. Yu, Y. Zeng, W. Huang, X. Hao and W.-H. Sun, *Dalton Trans.*, 2011, **40**, 8436; (b) L. Zhang, X. Hao, W.-H. Sun and C. Redshaw, *ACS Catal.*, 2011, **1**, 1213; (c) X. Hou, Z. Cai, X. Chen, L. Wang, C. Redshaw and W.-H. Sun, *Dalton Trans.*, 2012, **41**, 1617.

16 F. Huang, Q. Xing, T. Liang, Z. Flisak, B. Ye, X. Hu, W. Yang and W.-H. Sun, *Dalton Trans.*, 2014, **43**, 16818.

17 J. H. Groen, M. J. M. Vlaar, P. Leeuwen, K. Vrieze and H. Kooijman, *J. Organomet. Chem.*, 1998, **551**, 67.

18 T. Xiao, P. Hao, G. Kehr, X. Hao, G. Erker and W. -H. Sun, *Organometallics*, 2011, **30**, 4847.

19 S. D. Ittel, L. K. Johnson and M. Brookhart, *Chem. Rev.*, 2000, **100**, 1169.

20 (a) D. Guo, L. Han, T. Zhang, W.-H. Sun, T. Li and X. Yang, *Macromol. Theory Simul.*, 2002, **11**, 1006; (b) D. Guo, X. Yang, T. Liu and Y. Hu, *Macromol. Theory Simul.*, 2001, **10**, 75; (c) D. Guo, X. Yang, L. Yang, Y. Li, T. Liu, H. Hong and Y. Hu, *J. Polym. Sci., Part A: Polym. Chem.*, 2000, **38**, 2232.

21 G. B. Galland, R. F. Souza, R. S. Mauler and F. F. Nunes, *Macromolecules*, 1999, **32**, 1620.

22 (a) K. Song, W. Yang, B. Li, Q. Liu, C. Redshaw, Y. Li and W. -H. Sun, *Dalton Trans.*, 2013, **42**, 9166; (b) S. Kong, C. -Y. Guo, W. Yang, L. Wang, W. -H. Sun and R. Glaser, *J. Organomet. Chem.*, 2013, **725**, 37.

23 (a) L. C. Simon, R. S. Mauler and R. F. Souza, *J. Polym. Sci., Part A: Polym. Chem.*, 1999, **37**, 4656 ; (b) G. J. P. Britovsek, M. Bruce, V. C. Gibson, B. S. Kimberley, P. J. Maddox, S. Mastroianni, S. J. McTavish, C. Redshaw, G. A. Solan, S. Stromberg, A. J. P. White and D. J. Williams, *J. Am. Chem. Soc.*, 1999, **121**, 8728; (c) G. J. P. Britovsek, S. A. Cohen, V. C. Gibson and M. Meurs, *J. Am. Chem. Soc.*, 2004, **126**, 10701.

24 G. M. Sheldrick, *SHELXTL-97 Program for the Refinement of Crystal Structures*, University of Göttingen, Germany, 1997.

25 L. Spek, *Acta Crystallogr. D: Biol. Crystallogr.*, 2009, **65**, 148.

Dalton Transactions Accepted Manuscript

Table of Content only

for

Ring-tension Ajusted Ethylene Polymerization by Aryliminocycloheptapyridylnickel Complexes

Fang Huang, Zelin Sun, Shizhen Du, Erlin Yue, Junjun Ba, Xinquan Hu, Tongling Liang, Griselda B. Galland, and Wen-Hua Sun*

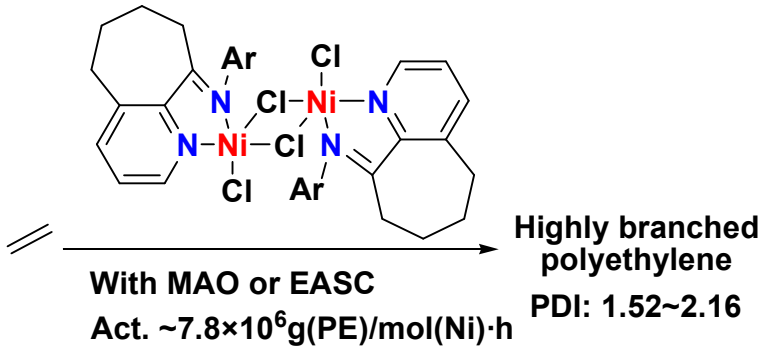

The 9-aryliminocyclo-heptapyridylnickel chlorides, activated by $Et_3Al_2Cl_3$ or MAO, exhibited high activities toward ethylene polymerization and produced highly branched PE in narrow polydispersity.

Dalton Transactions Accepted Manuscript